New Equipment Designs for Evaluation of Fade Stability of Color Photographic Images in the Presence of Ozone Gas – Part One

David Miller, Eastman Kodak Company, Rochester NY, USA

Abstract

The Image Stability Technical Center of Eastman Kodak Company is evaluating various media in a newly designed system for testing image permanence in the presence of elevated levels of ozone. This initial paper will discuss experiments designed to look at chamber performance and within chamber exposure uniformity. Results from the first experimental run are included. Future studies will include media type, gas volume/velocity, impingement method, and reciprocity effects over a 10:1 range of concentration.

Introduction

It is well documented that exposure to the common air contaminant ozone is one of the more important factors impacting the life of printed images.[1] With this recognition, the digital print industry has been working toward the goal of adopting a standardized test method for establishing image permanence claims based on ozone exposure. Consensus on methodology is sometimes hampered by the lack of test data and need for further study.

Commercially available environmental chambers used in ozone testing can be costly and may afford only limited experimental flexibility because of fundamental capabilities or as-manufactured design impediments.

Eastman Kodak Company has just completed development of a custom environmental chamber (Fig. 1) for dedicated use in understanding and quantifying the impact of ozone exposure on printed images.

In addition to controlling temperature, humidity, and ozone concentration, this new chamber affords the ability to study other variables such as impingement method and velocity. Key parameters are monitored and controlled using a programmable logic controller. Refer to Fig. 2 for general design.

The chamber design employs a variable speed centrifugal blower to regulate the air volume being recirculated. Impingement velocity is controlled via fan speed, the design of the perforation pattern in the impingement plenum, and the target standoff distance. Fig. 3 pictures one style of impingement plenum.

Fig. 1: New ozone environmental chamber from Eastman Kodak Company.

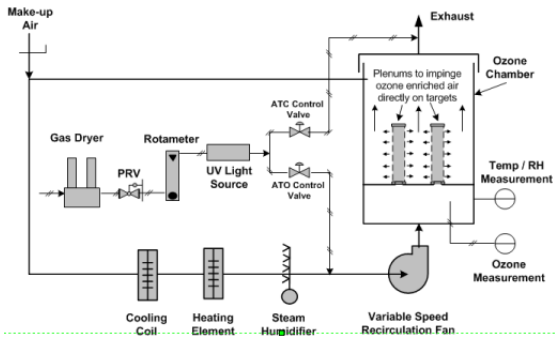

Fig. 2: Chamber design schematic.

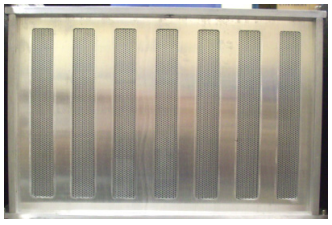

Fig. 3: Face of impingement plenum.

A UV light source is utilized to generate ozone, which eliminates potential contamination from the by-products associated with ozone generation using the corona discharge method. Ozone concentration as supplied to the targets is measured within the chamber and is precisely controlled by continuously regulating the position of two control valves, either directing ozone-enriched instrument air to the chamber or to exhaust. Ozone enters the chamber at the inlet of the centrifugal fan to achieve good mixing. The air in the room where the chamber resides is scrubbed using carbon filters to reduce ambient ozone concentration to ~2 ppb. A small amount of continuous exhaust ensures that some fresh make-up air is continually introduced into the chamber to avoid build-up of any potential contaminants.

1. Experiment

This initial experiment examined the uniformity of fade results over a set of identical targets at typical conditions of 22.2 ºC (72 F) dry bulb, 50% RH and an elevated ozone concentration of 1 ppm, all under closed loop control at two impingement velocities (condition 1 and condition 2 in the following). In the chamber, all test targets were equally spaced off impingement plenums using fixed position target mounts. Ozone-enriched air was impinged at 90º to every target face. Ozone concentration supplied to the targets was held constant for the experiment duration, except for very brief periods of recovery after initial loading and at measurement intervals.

The following equipment was used in this initial ozone exposure uniformity trial:

- InUSA IN-2000 LoCon UV adsorption ozone analyzer
- General Eastern Hygro M2 hygrometer
- Gretag Macbeth/Spectroscan densitometer
- Kodak's custom designed environmental chamber as described above

Temperature and humidity conditions were confirmed prior to the start of the experiment using a hygrometer with traceable calibration. Ozone concentration was measured with an InUSA ozone analyzer with traceable calibration and confirmed with a redundant analyzer. Conditions were monitored and confirmed throughout the experiment duration.

For this first uniformity experiment, the media chosen employed dye-based inks on porous photo paper. The particular system chosen was thought to have a high sensitivity to ozone exposure. A test target was designed having 18 patches each of neutral, magenta, and cyan, all at respective equal d_{max} densities, as shown in Fig. 4. Three neutral d_{min} patches are also included. (Prior testing has revealed that magenta and cyan are typically the first colors to fail when exposed to ozone.)[1]

Fig. 4: Test target.
(57 blocks, neutral d_{max} on left, magenta center, cyan on right, neutral d_{min} on bottom)

For this initial experiment, d_{max} targets were used to maximize the potential for ozone adsorption and create a worst-case test scenario for evaluation of the new chamber. Fresh samples were printed just prior to the start of the experiment from the same lot of paper and ink and allowed to age for five days before taking initial density measurements using the Gretag Spectroscan densitometer. Subsequent measurements after exposure were taken at four and 13 days.

Test targets were held on three sides in a frame for precise and constant positioning throughout the experiment. A target blade having seven mounted targets on one face is shown in Fig. 5. This mount allowed for only single-sided target exposure to ozone during the experiment. In total, 70 targets were mounted in the chamber (ten rows front to back, seven columns across).

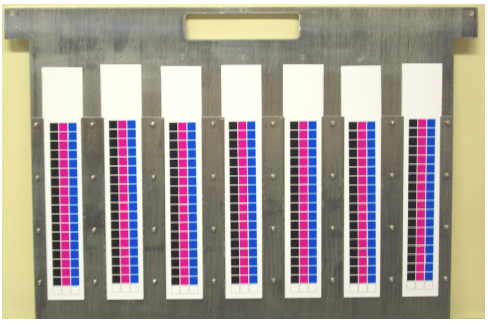

Fig. 5: Target mounting blade with targets.

Results and Discussion

Condition One – 95 fpm impingement velocity

Chamber Conditions (95 fpm)

Fig. 6 shows a typical trend of dry bulb and wet bulb conditions captured over a four-day period during the experiment, reflecting stable control at 22.2 ºC (75 F) and 50%.

Dry bulb statistics for the entire experiment include a mean average of 22.2 ºC, a range of 0.2 ºC and one standard deviation of 0.073 ºC.

Wet bulb statistics for the entire experiment include a mean average of 15.6 ºC, a range of 1.1 ºC and one standard deviation of 0.171 ºC.

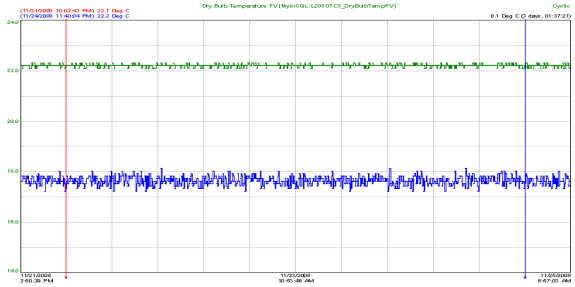

Fig. 6: Dry bulb/wet bulb temperature control.

Ozone Recovery/Conditions (95 fpm)

Fig. 7 is a trend chart of the ozone recovery to a 1 ppm set point after the chamber was initially loaded with 70 fresh targets. The chamber was back in control at 1 ppm within 20 min (bold red line.)

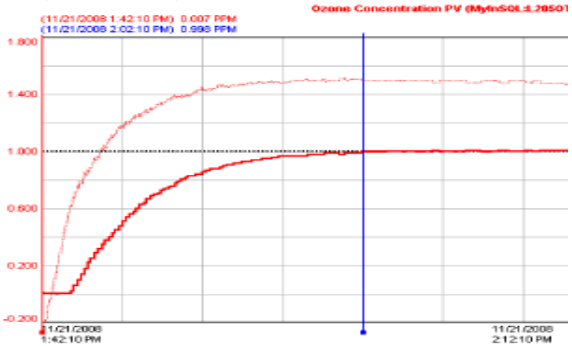

Fig. 7: Ozone recovery after initial load.

Fig. 8 reflects the decreasing output to the ozone control valves required to maintain a 1 ppm concentration in the chamber, as the sample targets came into equilibrium during the first 24 h of the test (decaying light red line). For the remainder of the test, the output settled in at a value just slightly higher than that required to maintain the 1 ppm concentration in a chamber totally empty of targets.

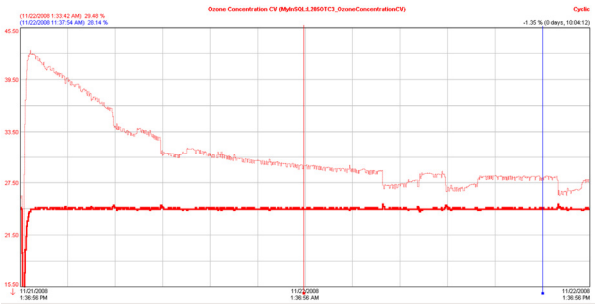

Fig. 8: Ozone stabilization.

Ozone Control (95 fpm)

Fig. 9 shows a typical trend of ozone control at 1 ppm captured over a seven-day period during the course of the experiment.

Ozone control statistics for the full experiment include a mean average of 1.0 ppm, a range of 0.054 ppm, and one standard deviation of 0.007 ppm.

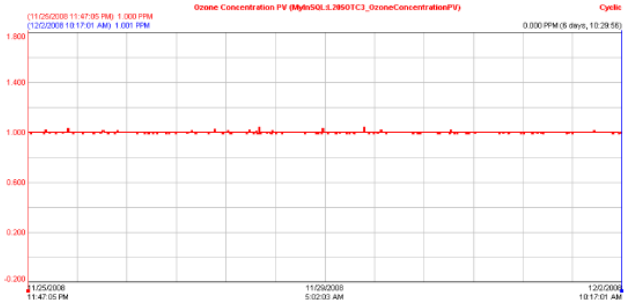

Fig. 9: Ozone control.

Ozone Exposure Uniformity (95 fpm)

Two different impingement velocities were included in this study. The first condition was set up to yield a bulk impingement velocity of ~95 fpm. From earlier experiments, it was theorized that at some impingement velocity, the ozone-driven fade reaction would become "rate limited" – at this condition, the fade reaction becomes insensitive to further increases in velocity and achieves a stable plateau for a given exposure duration.

While all patches from all 70 strips were read, only a top, middle, and bottom row of each strip were compared to simplify the analysis for this report. Analysis is based on comparing differential target densities from the day 13 readings after targets were removed to the day 0 readings at initial loading. Changes are reported as density loss (△D).

Data from the first condition (72 F/50%, 1 ppm and 95 fpm) is summarized in Table 1. These data include the same top, middle, and bottom target patches from all 70 strips for the cyan, magenta, and neutral D_{max} records.

	includes all 70 targets									
	Cyan		Magenta		Neutral					
	[red channel]		[green channel]		[red channel]		[green channel]		[blue channel]	
	Ave.	Std Dev	Ave.	Std Dev	Ave.	Std Dev	Ave.	Std Dev	Ave.	Std Dev
Top	-0.23	0.03	-0.31	0.02	-1.30	0.04	-0.60	0.05	-0.20	0.07
Middle	-0.23	0.03	-0.28	0.02	-1.32	0.04	-0.61	0.05	-0.19	0.07
Bottom	-0.24	0.03	-0.33	0.02	-1.34	0.03	-0.63	0.04	-0.22	0.07

Table 1: Condition One – all 70 targets.

The range of standard deviations for this data (0.02 to 0.07) is much higher than desired and indicates some degree of nonuniformity in the chamber. A closer analysis of the data revealed that the outside rows and columns were contributing to most of the variability, likely due to edge effects within the chamber.

Removal of all the data from the first and last rows and for columns A and G in all rows leaves only the center 40 targets remaining. This data subset is summarized in Table 2.

	subset of 40 center targets (all outside targets eliminated)									
	Cyan		Magenta		Neutral					
	[red channel]		[green channel]		[red channel]		[green channel]		[blue channel]	
	Ave.	Std Dev	Ave.	Std Dev	Ave.	Std Dev	Ave.	Std Dev	Ave.	Std Dev
Top	-0.22	0.02	-0.30	0.02	-1.28	0.03	-0.58	0.02	-0.17	0.02
Middle	-0.22	0.01	-0.28	0.01	-1.31	0.02	-0.59	0.02	-0.16	0.02
Bottom	-0.23	0.01	-0.32	0.01	-1.33	0.02	-0.62	0.02	-0.20	0.01

Table 2: Condition One – Center 40 targets only.

The data from these center 40 targets are much more uniform, yielding a significantly smaller and more acceptable range of standard deviations (0.01 to 0.03) across all channels. At this range of standard deviation, the differential densities represent a much-improved signal for interpretation.

Condition Two – 165 fpm impingement velocity

Chamber Conditions (165 fpm)

For this second part, chamber performance statistics were similar to that of part 1 and do not bear repeating. Fig. 10 shows the trend data for dry bulb, wet bulb, and ozone concentration.

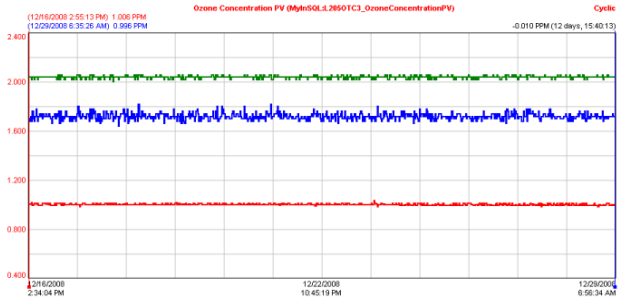

Fig. 10: Condition 2 chamber trends.

Ozone Recovery and Stabilization (165 fpm)

Fig. 11 depicts the ozone recovery to 1 ppm after initial startup (bold red curve) and the ozone control output stabilization (light red curve) within the first 12 h. As in the first condition, the concentration was at 1 ppm within 20 min, but the stabilization of the loop output was much faster with the higher impingement velocity.

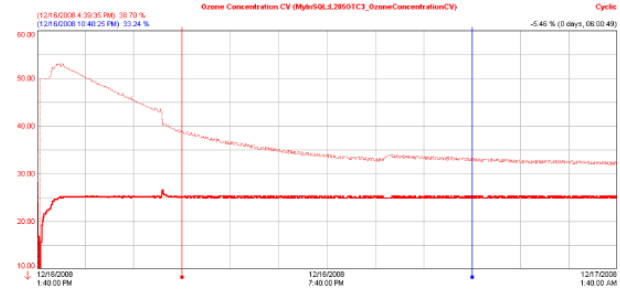

Fig. 11: Condition 2 – Ozone recovery/stabilization.

Ozone Exposure Uniformity (165 fpm)

Data from the first condition suggested we had not reached the stable plateau discussed earlier in this article. Therefore, this second condition was conducted at a bulk impingement velocity of ~165 fpm, while maintaining the 90º target impingement with identical chamber conditions and media targets. It was anticipated that more fade would be evident but with the hope that substantially more uniform results would be seen in all target positions and patches.

Initial examination of these data does indicate the higher levels of fade anticipated. However, this new data set does not show the significant improvement in uniformity sought. More analysis and testing are needed before final conclusions can be drawn regarding impingement velocity effects.

	subset of 40 center targets (all outside targets eliminated)									
	Cyan		Magenta		Neutral					
	[red channel]		[green channel]		[red channel]		[green channel]		[blue channel]	
	Ave.	Std Dev	Ave.	Std Dev	Ave.	Std Dev	Ave.	Std Dev	Ave.	Std Dev
Top	-0.30	0.02	-0.37	0.01	-1.36	0.05	-0.67	0.04	-0.26	0.02
Middle	-0.28	0.02	-0.33	0.02	-1.35	0.04	-0.66	0.04	-0.21	0.03
Bottom	-0.30	0.03	-0.37	0.02	-1.36	0.05	-0.68	0.05	-0.25	0.03

Table 3: Condition 2 – center 40 targets.

Conclusions/Future Studies

Chamber conditions

The accuracy and precision of dry bulb temperature and ozone control at this test condition are very acceptable. Wet bulb accuracy is also very acceptable and precision could likely be improved with additional emphasis on loop tuning parameters. This improvement has subsequently been demonstrated after the conclusion of this first experiment.

Other chamber conditions will be evaluated as experimental designs dictate.

Exposure Uniformity

Without some internal design changes, it is recommended that only the center 40 positions be used for future analysis. Executing larger and more complex experiments requiring more than 40 targets will necessitate some simple internal chamber redesign to improve uniformity along the edges.

Impingement Velocity

Without further analysis, data from this first experiment does not initially suggest we reached a velocity where fade results would be at a stable plateau. As we continue exploring chamber performance, we will be investigating other impingement velocities as well as contrasting to more traditional low-velocity flooded chamber lab-scale units available in the Kodak Research Laboratories.

Future Studies

The immediate focus of our early experiments will be on improving chamber performance and understanding the effects of impingement velocity and angle.

Future evaluations will involve ozone concentration reciprocity factors and temperature/humidity effects. These experiments are expected to include additional media types representative of industry products (e.g., dyes/pigmented inks, porous/swellable media, and thermal) and will utilize a more comprehensive media target design with respect to color science.

References

[1] D. Bugner, R. Van Hanehem, M. Oakland, P. Artz, D. Zaccour, and R. Levesque, *Ozone Concentration Effects on the Dark Fade of Ink Jet Photographic Prints,* JIST, Vol. 49, No. 6, 2005.

Author Biography

David (Dave) Miller is a senior research engineer at Eastman Kodak Company. He received his B.S. in mechanical engineering from Clarkson College of Technology in 1974. In 1999, Mr. Miller was accredited as a Six Sigma black belt quality practitioner. Since joining Kodak, he has held roles as a mechanical design engineer, project manager, process engineer, operations supervisor, maintenance engineer, and most recently, quality engineer for the Image Stability Technical Center, Consumer Digital Group, Eastman Kodak Company.

References/bibliography of interest from the above reference, with acknowledgement to the author:

- E. Zinn, E. Nishimura and J. Reilly, Proc. IS&T's NIP 15, IS&T, Springfield, VA, 1999, pp. 416–420.
- S. Schuttel and R. Hofmann, Proc. IS&T's NIP 15, IS&T, Springfield, VA, 1999, pp. 120–123.
- D. E. Bugner and C. Suminski, Proc. IS&T's NIP 16, IS&T, Springfield, VA, 2000, pp. 90–94.
- S. Guo and N. Miller, Proc. IS&T's NIP 17, IS&T, Springfield, VA, 2001, pp. 186–191.
- H. Onishi, M. Hanmura, H. Kanada, and T. Kaieda, Proc. IS&T's NIP 17, IS&T, Springfield, VA, 2001, pp. 192–96.
- H. Wilhelm and M. McCormick-Goodhart, Proc. IS&T's NIP 17, IS&T, Springfield, VA, 2001, pp. 197–202.
- G. Van Ackere, H. Kanora, M. Graindourze, H. Friedel, and S. Lingier,Proc. IS&T's NIP 17, IS&T, Springfield, VA, 2001, pp. 213–17.
- B Vogt and F. Frey, Proc. IS&T's NIP 17, IS&T, Springfield, VA, 2001, pp. 218–21.
- R. Steiger, P.-A. Brugger, and M. Staiger, Proc. IS&T's NIP 17, IS&T,Springfield, VA, 2001, pp. 222–25.
- B. Vogt, Stability Issues and Test Methods for Ink Jet Materials, Thesis,Department of Image Engineering, University of Applied Science,Cologne, Germany, 2001.
- D. E. Bugner, D. Kopperl, and P. Artz, Proc. IS&T 12th Int. Symp. On Photofinishing, IS&T, Springfield, VA, 2002, pp. 54–57.
- H. Onishi, H. Kanada, T. Sano, and K. Takemoto, Proc. IS&T's NIP 18, IS&T, Springfield, VA, 2002, pp. 315–318.
- E. Burch, A. Kabalnov, N. Miller, C. Dupuy, B.-J. Niu, P. Wang, S. Guo, P. Tyrell and L. Deardurff, Proc. IS&T's NIP 18, IS&T, Springfield, VA, 2002, pp. 342–347.
- P. Hill, K. Suitor, and P. Artz, Proc. IS&T's NIP 16, IS&T, Springfield, VA, 2000, pp. 70–73.
- M. McCormick-Goodhart, Proc. IS&T's NIP 16, 2000, pp. 74–77.
- M. Oakland, D. E. Bugner, R. Levesque, and P. Artz, Proc. IS&T's NIP 17, IS&T, Springfield, VA, 2001, pp. 167–70.
- M. McCormick-Goodhart and H. Wilhelm, Proc. IS&T's NIP 17, IS&T, Springfield, VA, 2001, pp. 179–185.
- S. Guo, N. Miller, and D. Weeks, Proc. IS&T's NIP 18, IS&T, Springfield, VA, 2002, pp. 319–325.
- M. Oakland, D. E. Bugner, R. Levesque, and R. Vanhanehem, Proc. IS&T's NIP 17, IS&T, Springfield, VA, 2001, pp. 175–178.
- D. Sid, Proc. IS&T's NIP 17, IS&T, Springfield, VA, 2001, pp. 171–174.
- K. Kitamura, H. Hayashi, and Y. Oki, Proc. ICIS '02, SPSTJ, Tokyo, Japan, 2002, pp. 539–542.
- P. Wight, Proc. IS&T's NIP 18, IS&T, Springfield, VA, 2002, pp.334–336.
- M. Thornberry and S. Looman, Proc. IS&T's NIP 19, IS&T, Springfield, VA, 2003, pp. 426–430.
- R. H. Sabersky, D. A. Sinema and F. H. Shair, Environ. Sci. Tech.**7**(4), 347–353 (1973).
- F. H. Shair and K. L. Heitner, Environ. Sci. Tech. **8**(50), 444–451 (1974).
- J. E. Yocum, J. Air Pollution Control Assoc. **32**(5), 500–520 (1982).
- T. D. Davies, B. Ramer, G. Kaspyzok, and A. C. Delany, J. Air Pollution Control Assoc. **31**(2), 135–137 (1984).
- T. Jones, J. Soc. Dyers Colourists **52,** 291 (1936).
- F. M. Rowe and K. A. J. Chamberlain, J. Soc. Dyers Colourists **53,** 268–278 (1937).
- J. M. Straley and J. B. Dickey, U.S. Patents 2,641,602 and 2,651,641 (1953).
- V. S. Salvin and R. S. Walker, Text. Res. J. **25**(7), 571 (1955).
- N. J. Beloin, Text. Chem. Color **5**(7), 128–151 (1973).
- V. S. Salvin, Text. Chem. Color **6**(8), 185–189 (1974).
- J. C. Haylock and J. L. Rush, Textile Res. J. **56,** 1–8 (1976).
- J. S. Arney, A. J. Jacobs, and R. Newman, JAIC **18,** 108–117 (1979).
- T. Aono, K. Nakamura, and M. Furutachi, J. Applied Photogr. Eng. **8,** 227–231 (1982).
- The Hardcopy Supplies Journal, **7**(1), 25 (2001).
- D. E. Bugner and P. Artz, Proc. ICIS '02, SPSTJ, Tokyo, Japan, 2002, pp. 308–310; (b) D. E. Bugner and P. Artz, Proc. IS&T's NIP 18, 2002, pp. 306–309.
- Y. Shibahara, H. Ishizuka, N. Muro, Y. Kanazawa, and Y. Seoka, Proc. IS&T's NIP 18, IS&T, Springfield, VA, 2002, pp. 330–333.
- ANSI IT9.9 (1996); (b) ASTM F2035 (2000); and (c) ASTM F2037 (2000).